

IDENTIFICATION OF HIGH NOISE ZONES WITH A 3D PILE DRIVING NOISE MODEL

Jonas von Pein, Elin Klages, Stephan Lippert, Otto von Estorff

Hamburg University of Technology (TUHH), Institute of Modelling and Computation,
Denickestr. 17, 21073 Hamburg, Germany, [mailto: mub@tuhh.de](mailto:mub@tuhh.de)

Abstract: *Piles are the state-of-the-art technology for fastening the foundations of offshore wind power plants to the sea-floor. Due to the ongoing construction and development of offshore wind farms, pile driving activities at sea are increasing. During the piling process high noise levels are emitted into the water. These levels are potentially harmful for the marine environment, wherefore limits for the noise levels apply. These limits can be complied with by the use of noise mitigation systems, e.g., bubble curtains. In order to assess, if such systems are needed, detailed pile driving noise models for the prediction of the underwater noise emissions are necessary. Typical pile driving noise models are based on the finite-element-method (FEM) for ranges up to 1 km and coupled to a far-field model for distances further away from the pile. The FE-models are set up rotationally symmetric. Therefore, only small changes of the bathymetry can be accounted for. In order to consider 3D-effects induced by a varying bathymetry, e.g. a full 3D parabolic equation (PE) model can be used for the far-field computation. At a construction site with a variable water depth, the identification of hydrophone locations for noise monitoring is not straightforward. Therefore, zones with high noise levels have to be identified in a reliable way. Within this contribution results of pile driving noise computations for a real-life future pile driving scenario with a heavily changing bathymetry are shown. In the final step, the possibility of finding these high noise zones by the examination of the transmission loss plot of a point source is examined.*

Keywords: *Pile Driving, Underwater Noise, Parabolic Equations, Finite Element Method, 3D-Modelling*

1. INTRODUCTION

Offshore infrastructures, e.g. offshore wind power plants, are mainly fastened to the sea-floor by piles. Percussive pile driving is commonly used to bring the pile to the final penetration depth and can be considered as the state-of-the-art technique. Each hammer strike induces a compressional wave running down the pile, being reflected at both ends and running up and down again until its energy is dissipated. This wave leads to radial deformations of the pile, which excite pressure waves into the water as well as compressional and shear waves into the soil. The resulting wave fronts and their interference lead to high sound pressure levels in the water, which are potentially harmful for the marine fauna, e.g. the harbour porpoise [1]. In order to protect the marine environment, limits for the sound levels apply in several countries. For instance, in the German Exclusive Economic zone, the limits are set at 750 m as 160 dB for the sound exposure level (SEL) and 190 dB for the peak sound pressure level (SPL_{peak}) [2]. The SEL and SPL_{peak} are computed with the time pressure series $p(t)$ by

$$\text{SEL} = 10 \log_{10} \left(\frac{1}{T_0} \int_0^\infty \frac{p(t)^2}{p_0^2} dt \right) \text{dB} \quad (1)$$

and

$$\text{SPL}_{\text{peak}} = 10 \log_{10} \left(\frac{\max(p(t)^2)}{p_0^2} \right) \text{dB} \quad (2)$$

where $p_0 = 1 \mu\text{Pa}$ and $T_0 = 1\text{s}$. To assess the sound levels prior to construction, accurate predictions of the sound pressure levels are necessary. These predictions can be performed with numerical or analytical models. Thereby, the advantages of detailed numerical models are the possibility of optimizing the pile driving set-up, e.g., the hammer, and the revision of the necessary noise mitigation concept. Furthermore, a high physical insight regarding noise transmission and propagation is given.

One of the first modelling approaches has been suggested by Reinhall and Dahl [3]. Meanwhile, several researchers have developed their own approaches and many of them presented their methods at the benchmarking workshops COMPILE I and II [4], [5]. All of the applied models therein assumed a bathymetry that can be considered as rotationally symmetric. However, 3D-effects may have an influence on the sound pressure levels at locations with heavily changing bathymetries. In order to be able to take 3D-effects into account, a hybrid 3D pile driving noise model has been developed by the authors [6].

The hydrophones for the measurement of the occurring sound pressure levels are usually placed at 750 m and 1500 m [2]. If the bathymetry is flat, there are only small differences in the measurement results at hydrophone locations with different azimuthal angles ϕ and a constant range. However, if the bathymetry is heavily changing, the positioning and the computation of the sound pressure levels at these distances is not straightforward. Therefore, this contribution focusses on the identification of high noise levels at the different measurement distances. This is done with full 3D- and Nx2D-computations of the SEL and tried with the transmission loss (TL) plots of a point source. For the investigations a real-life pile driving scenario is used. The measurement data of the heavily changing bathymetry of the considered scenario is shown in fig. 1.

This contribution is organized as follows: First, the used modelling approach is briefly described. Second, the main details of the considered real-life pile driving scenario are listed and the high-noise zones at the measurement ranges are identified by full 3D- and Nx2D-computations and the differences between them are investigated. Finally, it is examined if the

high-noise zones can also be identified with the TL plots of a point source with a frequency of 100 Hz placed in the middle of the water column.

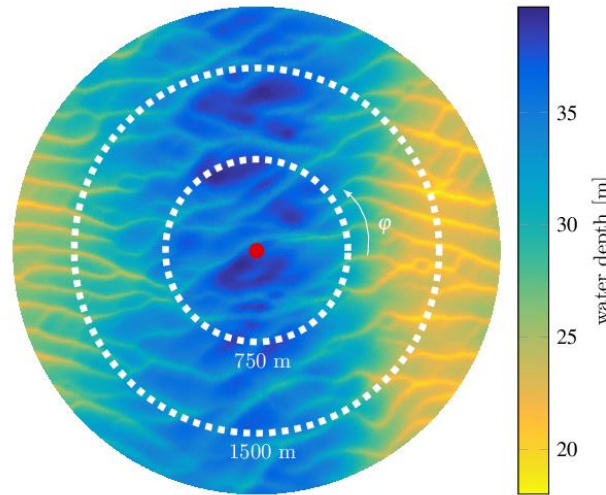


Fig.1: Measured bathymetry at the considered real-life pile driving location.

2. MODELLING APPROACH

The applied model is based on a hybrid modelling approach using the finite element method (FEM) for the close-range and a parabolic equation (PE) model for the far-field computation. With the PE model, Nx2D- and 3D-solutions can be computed. The necessary starting field is directly derived out of the results of the FE model. A detailed description and a validation of this modelling approach for a 2D pile driving scenario are given in [6].

The FE model is rotationally symmetric and computed in time domain. It is split into a pre-calculation and the main acoustical model. Within the pre-calculation, only the interaction between pile and hammer is considered. Therein, all hammer parts, which are relevant for the resulting impulse, e.g. ram mass, anvil, and anvil ring, are accurately discretized. Together with the pile, the pile head excitation can be computed, which is used later on as a boundary condition within the main acoustical model. The main acoustical model consists of the pile, the water column, and a linear-elastic layered soil profile. At the sea-surface, a zero-pressure boundary condition is used, while non-reflecting boundary conditions are applied at all other edges of the domain. A detailed description of the FE model is given in [7], [8]. The same approach is also used in another contribution within these proceedings [9].

The 3D far-field model is based on the split-step Padé technique, which was first introduced by Collins [10]. It is implemented in a cylindrical coordinate system. The exactness of the 3D computation highly depends on the approximation of the square root in eq. 3. With the identity matrices I , the depth-operator X , and the azimuthal-operator Y , the considered Taylor expansion of the square root is

$$\sqrt{I + X + Y} \cong -I + \sqrt{I + X} + \sqrt{I + Y}. \quad (3)$$

In this case occurring cross-terms are neglected. The depth operator X is computed according to [11] and an eighth-order central-difference scheme for the azimuthal operator Y is used, as introduced by Sturm et al. [12]. A stair-step approximation is employed for the occurring sloping bottoms and the higher order energy conserving PE formulation is used [11].

The resulting range marching procedure consists of two steps: First, the pressure at the next range step $r+\Delta r$ is computed for every considered azimuthal direction. Second, the one-way wave equation with the azimuthal operator is solved and the outgoing field is corrected by taking horizontal diffraction into account. A detailed description of these two steps are also given by Lin et al. [13] for a Cartesian coordinate system.

3. IDENTIFICATION OF HIGH NOISE ZONES

The considered pile is a conical monopile with a diameter of 8.7 m, an averaged constant wall thickness of 81 mm, an overall length of 69 m, and a penetration depth of 32 m. The used hammer is an IHC S-3000 at a strike energy of 2000 kJ. The water-depth is shown in fig. 1. In the following, this unmitigated pile driving scenario is used to show the identification of high-noise zones.

In order to identify the highest sound pressure noise levels at the distances of 750 m and 1500 m, the SEL is evaluated at these ranges with an Nx2D- and a 3D-computation. The corresponding results are shown in fig. 2. The results are evaluated up to a depth of 40 m, whereas the actual water depth is indicated by a black line.

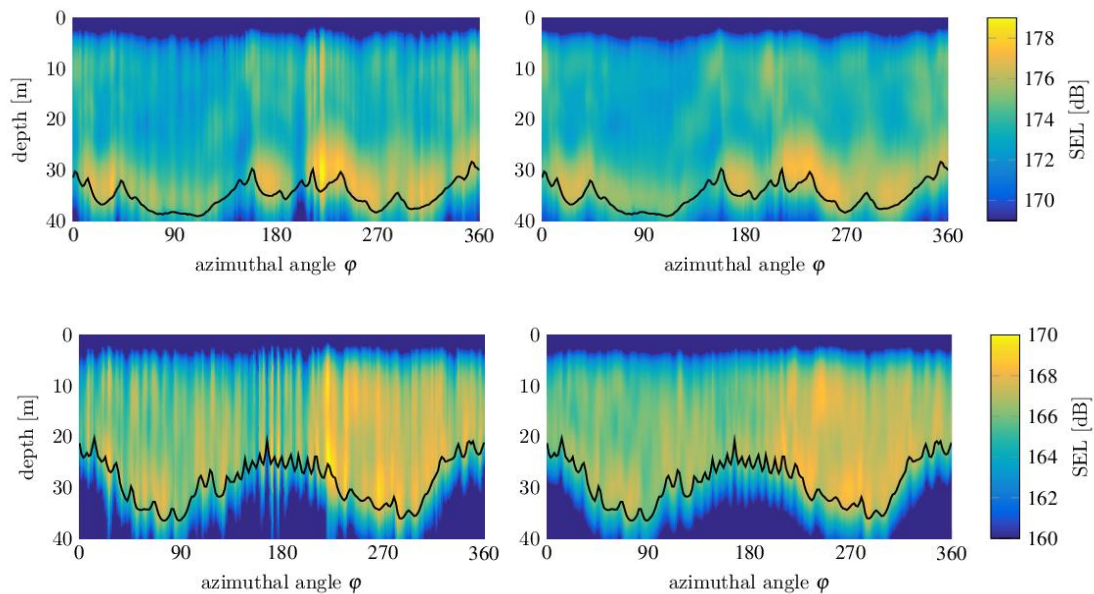


Fig.2: The 3D- (left) and Nx2D-results (right) of the SEL over depth and azimuth at 750 m (upper) and 1500 m (lower) together with the according water depth (black line).

At both distances the distribution of the SEL of the 3D- and Nx2D-results qualitatively has the same pattern. The evaluation of the results at 750 m clearly shows the existence of a high-noise zone between 212° and 237° , with the overall maximum of the 3D-results being 179.2 dB at 220° , which is about 1.6 dB higher than the maximum of the Nx2D-results. Another important aspect is that for $\phi > 180^\circ$ the SEL is generally higher. This indicates that the measurement direction should be chosen in the down-pointing canyon direction, compare fig. 1. These findings are also valid for a distance of 1500 m. Once again, the maximum of the SEL can be found around 220° with a difference between the Nx2D- and 3D-results of 2.2 dB and a SEL that is generally higher at $\phi > 180^\circ$. Overall, the differences between the 3D- and Nx2D-results are in the range of ± 3.5 dB at a distance of 750 m and $+4.5$ to -6.5 dB at 1500 m.

To check, if the identified angle of 220° is a reliable measurement position, the results need to be revised, to see if there are heavy oscillations along the radial direction. Therefore, the SEL is depicted over depth and range for an azimuthal angle of 220° in fig. 3. Once again, differences can clearly be seen between the Nx2D- and 3D-results, with the 3D-results being generally higher. Moreover, the 3D-results clearly show that the SEL does not oscillate much at the measurement positions 750 ± 50 m and 1500 ± 50 m at 2 m above the sea-floor when considering a possible uncertainty of ± 50 m due to positioning inaccuracies of the submerged measurement system.

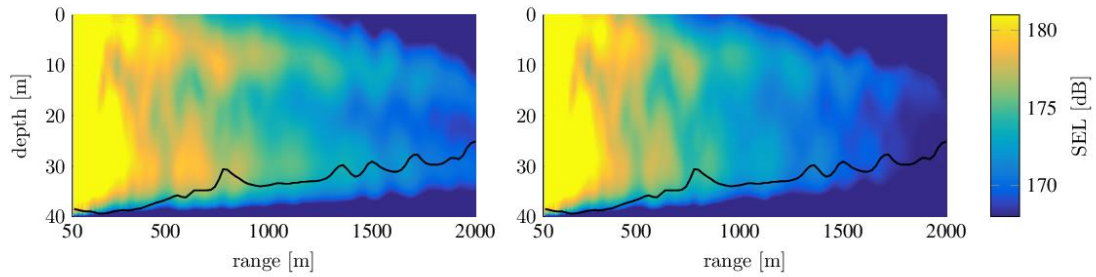


Fig.3: The 3D- (left) and Nx2D-results (right) of the SEL over depth and range at an azimuthal angle of $\varphi=220^\circ$.

In order to have a reliable identification of the high-noise zone, an evaluation of the SEL in the horizontal plane at 2 m above the sea-floor, which corresponds to water depths of 32 m for the 750 m position and 27 m for the 1500 m position, from $\varphi=180^\circ$ to $\varphi=360^\circ$ is shown in fig. 4. For a better physical insight, the bathymetry is indicated with black isolines. The contour of the bathymetry clearly shows the influence of the radial oriented sand dune close to the pile, which seems to evoke the comparably higher SEL in the identified high-noise zones. Furthermore, it can be observed that the high-noise zone is shaped like a ray with a width of about 100 m at the range of 1500 m.

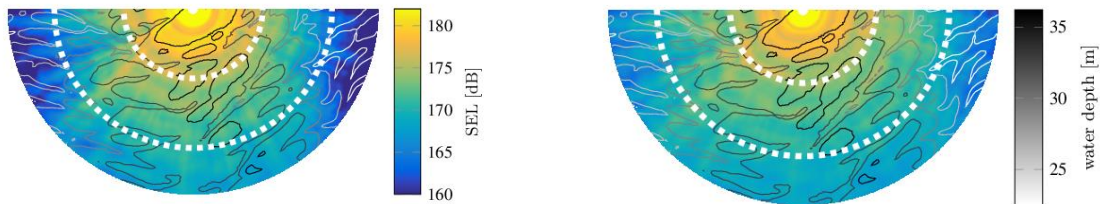


Fig.4: The 3D-results of the SEL evaluated at a corresponding water depth of 32 m (left) and 27 m (right) with the white circles at 750 m and 1500 m for $180^\circ \leq \varphi \leq 360^\circ$.

The evaluation of the SEL in different planes clearly showed, that a reliable high-noise zone has been identified at $\varphi=220$ and that there are locally big influences of 3D-effects on the sound pressure levels.

The energy of pile driving noise radiation is mainly concentrated around 100 Hz. In fig. 4 the transmission loss (TL) for the considered measurement ranges over depth and azimuth is shown when using a point source with 100 Hz placed in the middle of the water column instead of a vibrating pile.

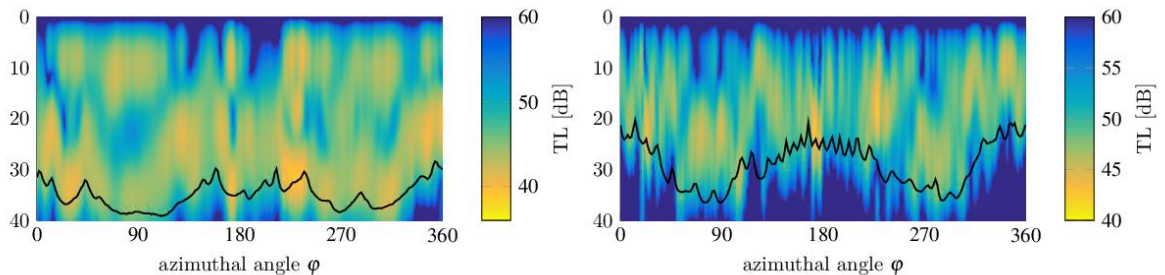


Fig.5: The 3D-results of the TL evaluated at 750 m (left) and 1500 m (right) of a point source with 100 Hz placed in the middle of the water column at 19 m below the sea-surface.

The results at 750 m clearly show a minimum of the TL at the identified high-noise zone around 220°. However, this finding cannot be reproduced for the distance of 1500 m, where none of the earlier identified effects can be seen. These results show that the TL plots of a single point source is not a valid measure to identify high-noise zones.

4. SUMMARY AND OUTLOOK

In this contribution the process of identifying high-noise zones at different measurement ranges for a pile driving location with a heavily varying bathymetry is shown. The comparison of the 3D- and Nx2D-results clearly indicated that Nx2D-computations are sufficient for a qualitative overview of high-noise zones, while full 3D-computations have to be conducted to get a good approximation of the highest sound pressure levels and the position of their occurrence. The comparison of the 3D- and Nx2D-results also showed that 3D-effects can locally lead to big differences in the considered sound pressure levels. Moreover, it can be observed that the radial-oriented sand dune close to the pile leads to higher noise levels at the measurement ranges. Furthermore, it is shown that high-noise zones can clearly be identified by evaluating the sound pressure levels in different planes and that these zones cannot be identified by only using a simplified point source representation as excitation.

The next step in the evolution of the presented 3D pile driving noise model is a validation with a real-life 3D pile driving case. Furthermore, the influence of uncertain parameters on the occurring 3D-effects and on the location of high-noise zones is going to be examined.

5. ACKNOWLEDGEMENTS

The authors would like to thank the company Ørsted Wind Power A/S for their friendly cooperation and valuable support.

REFERENCES

- [1] **R. A. Kastelein, R. Gransier, M. A. T. Marijt, and L. Hoek**, Hearing frequency thresholds of harbor porpoises (*Phocoena phocoena*) temporarily affected by played back offshore pile driving sounds, *J. Acoust. Soc. Am.*, vol. 137, no. 2, pp. 556–564, 2015.
- [2] **A. Müller and C. Zerbs**, “Offshore wind farms measuring instructions for underwater sound measurements. Current procedure application notes (Offshore-Windparks. Messvorschrift für Unterwasserschallmessungen. Aktuelle Vorgehensweise mit Anmerkungen. Anwendungshinweise), p. 39, 2011.
- [3] **P. G. Reinhall and P. H. Dahl**, Underwater Mach wave radiation from impact pile driving: theory and observation, *J. Acoust. Soc. Am.*, vol. 130, no. 3, pp. 1209–1216, 2011.
- [4] **S. Lippert, M. Nijhof, T. Lippert, D. Wilkes, A. Gavrilov, K. Heitmann, M. Ruhna, O. Von Estorff, A. Schäfer, I. Schäfer, J. Ehrlich, A. MacGillivray, J. Park, W. Seong, M. A. Ainslie, C. De Jong, M. Wood, L. Wang, and P. Theobald**, COMPILE - A Generic Benchmark Case for Predictions of Marine Pile-Driving Noise, *IEEE J. Ocean. Eng.*, vol. 41, no. 4, pp. 1061–1071, 2016.
- [5] **S. Lippert, O. von Estorff, M. J. J. Nijhof, and T. Lippert**, COMPILE II – A Benchmark of Pile Driving Noise Models against Offshore Measurements, in *Proceedings of Inter-Noise 2018, Chicago*, 2018.

- [6] **J. von Pein, E. Klages, S. Lippert, and O. von Estorff**, A hybrid model for the 3D computation of pile driving noise, in *Proceedings of OCEANS, Marseille*, 2019.
- [7] **S. Lippert, M. Huismann, M. Ruhnau, O. von Estorff, and K. van Zandwijk**, Prognosis of Underwater Pile Driving Noise for Submerged Skirt Piles of Jacket Structures, in *Proceedings of the UACE 2017 4th Underwater Acoustics Conference and Exhibition, Skiathos*, 2017.
- [8] **K. Heitmann, S. Mallapur, T. Lippert, M. Ruhnau, S. Lippert, and O. von Estorff**, Numerical determination of equivalent damping parameters for a finite element model to predict the underwater noise due to offshore pile driving, in *Proceedings of EuroNoise 2015, Maastricht*, 2015, pp. 605–610.
- [9] **E. Klages, J. von Pein, S. Lippert, and O. von Estorff**, An efficient model for offshore pile driving noise taking into account the hammer characteristics, in *Proceedings of the UACE 2019, 5th Underwater Acoustics Conference and Exhibition, Crete*, 2019.
- [10] **M. D. Collins**, A split-step Padé solution for the parabolic equation method, *J. Acoust. Soc. Am.*, vol. 93, no. 4, pp. 1736–42, 1992.
- [11] **M. D. Collins and E. K. Westwood**, A higher-order energy-conserving parabolic equation for range-dependent ocean depth, sound speed, and density, *J. Acoust. Soc. Am.*, vol. 89, no. 3, pp. 1068–1075, 1991.
- [12] **F. Sturm and J. a. Fawcett**, On the use of higher-order azimuthal schemes in 3-D PE modeling, *J. Acoust. Soc. Am.*, vol. 113, no. 6, pp. 3134–3145, 2003.
- [13] **Y.-T. Lin, J. M. Collis, and T. F. Duda**, A three-dimensional parabolic equation model of sound propagation using higher-order operator splitting and Padé approximants., *J. Acoust. Soc. Am.*, vol. 132, no. 5, pp. EL364-70, 2012.

